

Mobile Networks Connected Drones: Field Trials, Simulations, and Design Insights

Xingqin Lin, Richard Wiren, Sebastian Euler, Arvi Sadam, Helka-Liina Maattanen, Siva D. Muruganathan, Shiwei Gao, Y.-P. Eric Wang, Juhani Kauppi, Zhenhua Zou, and Vijaya Yajnanarayana

Ericsson

Contact: xingqin.lin@ericsson.com

Abstract— Drones are becoming increasingly used in a wide variety of industries and services and are delivering profound socioeconomic benefits. Technology needs to be in place to ensure safe operation and management of the growing fleet of drones. Mobile networks have connected tens of billions of devices on the ground in the past decades and are now ready to connect the flying drones in the sky. In this article, we share some of our findings in cellular connectivity for low altitude drones. We first present and analyze field measurement data collected during drone flights in a commercial Long-Term Evolution (LTE) network. We then present simulation results to shed light on the performance of a network when the network is serving many drones simultaneously over a wide area. The results, analysis, and design insights presented in this article help enhance the understanding of the applicability and performance of mobile network connectivity to low altitude drones.

I. INTRODUCTION

In this article, we focus on the applicability and performance of mobile network connectivity to low altitude drones. Drones have become increasingly important solutions considered among big retailers for deliveries such as the Amazon's Prime Air drone delivery service [1]. Besides deliveries, drones find applications in a wide variety of industries and services including infrastructure inspections and monitoring, photography and filming, precision agriculture, public safety, as well as coast guard and border control [2][3]. The growing fleet of drones are delivering profound socioeconomic benefits that are too large to be ignored [4].

To ensure safe operation and management of the growing

fleet of drones, technology needs to be in place to authenticate, monitor and control the drones, with connectivity support from backbone communications networks for command and control and payload communications [5]. Increasing efforts have been taken to meet this challenge. The Federal Aviation Administration (FAA) and National Aeronautics and Space Administration (NASA) have started a collaborative initiative to develop a drone traffic management system [6]. On October 25, 2017, the White House and U.S. Department of Transportation announced an innovative drone integration pilot program that aims to safely expand drone operations into the National Airspace by teaming up governments with drone operators [7]. New and exciting applications for connected drones have also attracted much academic attention, from channel modeling [8] to preliminary measurements [9] to connectivity management [10].

Mobile networks are well positioned to assist with drone traffic control and law enforcement [11]. As our results indicate, reusing existing ground-based mobile networks can facilitate the rapid growth of the drone ecosystem, without the need of developing completely new technologies and big network investments. To better understand the potential of mobile networks for low altitude drones, the 3rd Generation Partnership Project (3GPP) has dedicated a significant effort during its Release 15 to study enhanced Long-Term Evolution (LTE) support for aerial vehicles [12][13].

In our previous work [14], we have presented initial simulation results to shed light on the feasibility of using ground-based mobile networks for providing connectivity to

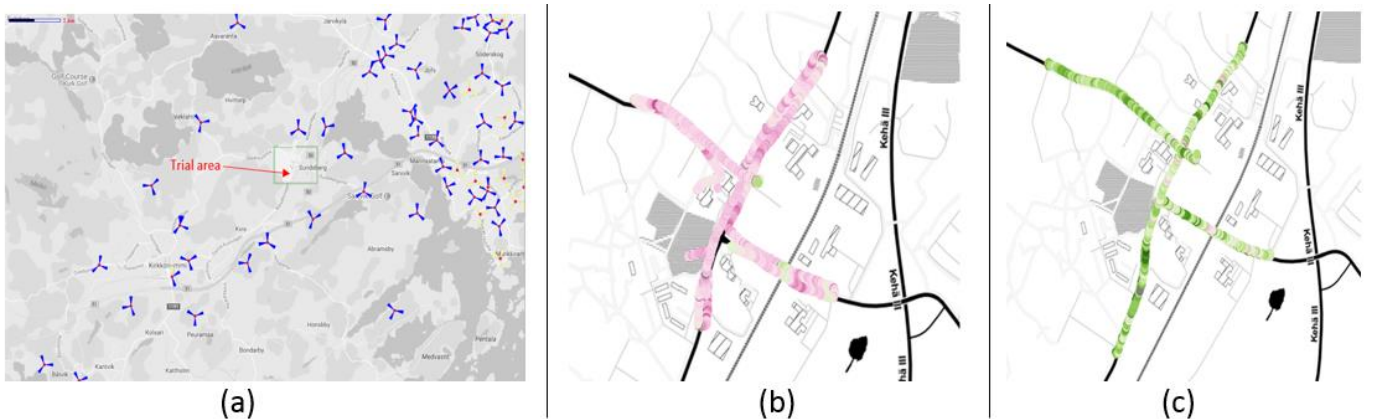


Figure 1: Drone flight test in Masala, Finland: (a) shows the positions of cell sites and the orientations of BS sector antennas around the test area; (b) shows the drone mobility route projected onto 2D map; (c) shows the reference mobility route of a car running on the ground.

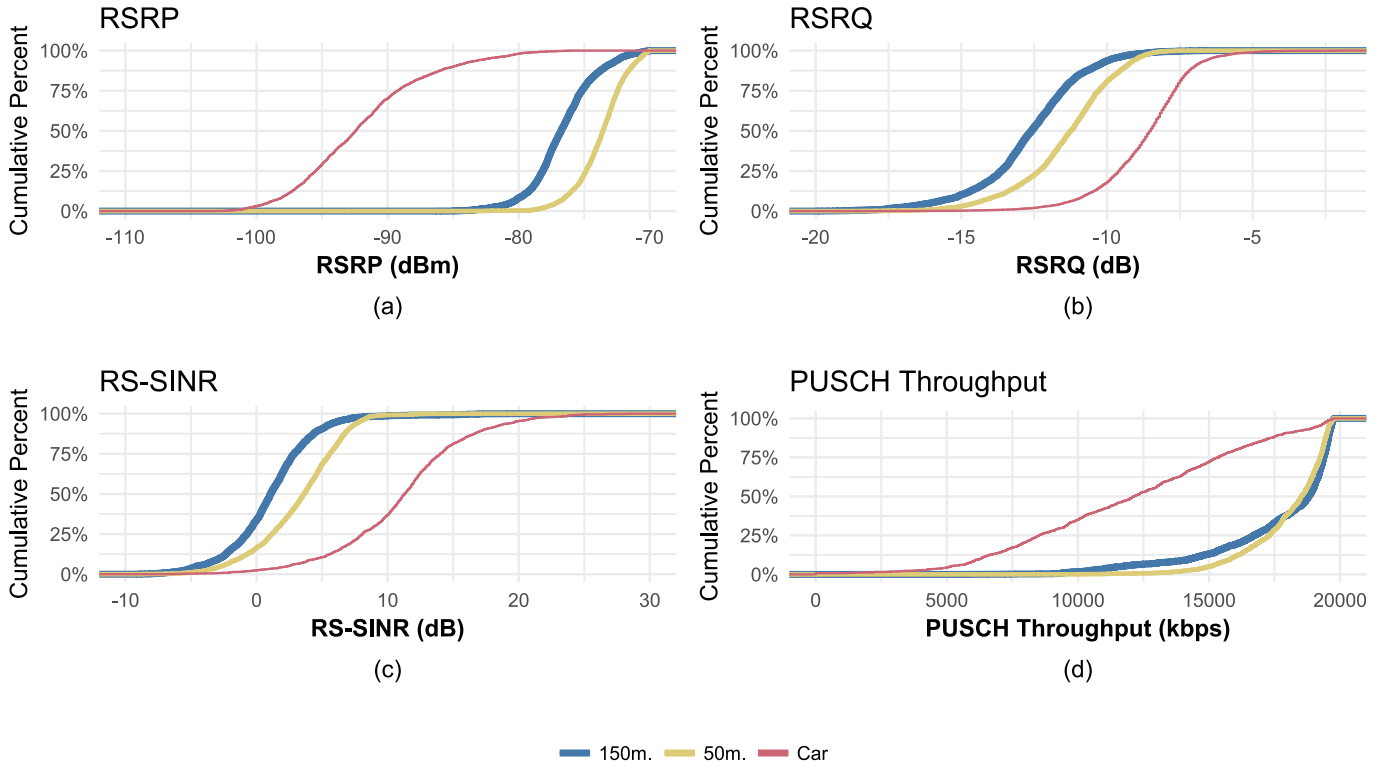


Figure 2: Serving cell measurement data: (a) shows distributions of RSRP; (b) shows distributions of RSRQ; (c) shows distributions of RS-SINR; (d) shows distributions of uplink throughput.

low-altitude drones. In this article, we share more of our findings in this field. We first present and analyze field trial measurement data collected during flights in a commercial LTE network. We then present further simulation results to study the network performance when the network is serving many drones simultaneously over a wide area. The results, analysis, and design insights presented in this article help enhance the understanding of the applicability and performance of mobile network connectivity to low altitude drones. We find that the existing mobile LTE networks targeting terrestrial usage can support the initial deployment of low altitude drones, but there may be challenges related to interference as well as mobility. Enhancements including those identified in the 3GPP technical report [13] and the next generation 5G networks will provide more efficient connectivity for wide-scale drone deployments.

II. FIELD TRIALS: MEASUREMENT SETUP

In this section, we describe measurement setup for the field measurement results collected in a commercial LTE network in a suburban area in Masala, Finland. Figure 1(a) shows the positions of cell sites and the orientations of sector antennas of base stations (BSs) around the test area.

Drone flights and measurements were performed by a consumer grade radio-controlled quadcopter: DJI Phantom 4 Pro. The maximum flight time of the drone is ~30 minutes. Measurement data were collected with a TEMS Pocket 16.3 installed on an LTE smart phone, which was mounted on the drone.

The results and analysis in later sections are derived from mobility routes on the ground, at 50 m height, and at 150 m height. The results collected on the ground serve as a baseline reference, and they were collected by driving a car on the ground along the mobility route shown in Figure 1(c). The drone mobility routes in the sky, shown in Figure 1(b) closely follow the mobility route on the ground. The flying speed of the drone was ~18 km/h. The driving speed of the car varied a bit (from 20 km/h to 40 km/h) due to traffic on the ground.

In Sections III and IV, we compare the measurement data collected in the sky to their counterparts collected on the ground. For the sake of brevity, we only present measurement data collected in 800 MHz band, though we measured other bands as well during the trials.

III. FIELD TRIALS: SERVING CELL RESULTS AND ANALYSIS

We start by looking at the field measurement data corresponding to the serving cell, as shown in Figure 2.

Reference signal received power (RSRP) is a key measurement parameter indicating the received power level in an LTE network. From the RSRP distributions in Figure 2(a), we can see that RSRPs at the heights of both 50 m and 150 m are higher than the RSRPs at ground level. The 50th percentile RSRPs at the heights of 50 m and 150 m are 18.9 dB and 15.6 dB higher than the corresponding value at ground level, respectively.

The commercial cellular network is equipped with down-tilted BS antennas to optimize terrestrial coverage. At the height

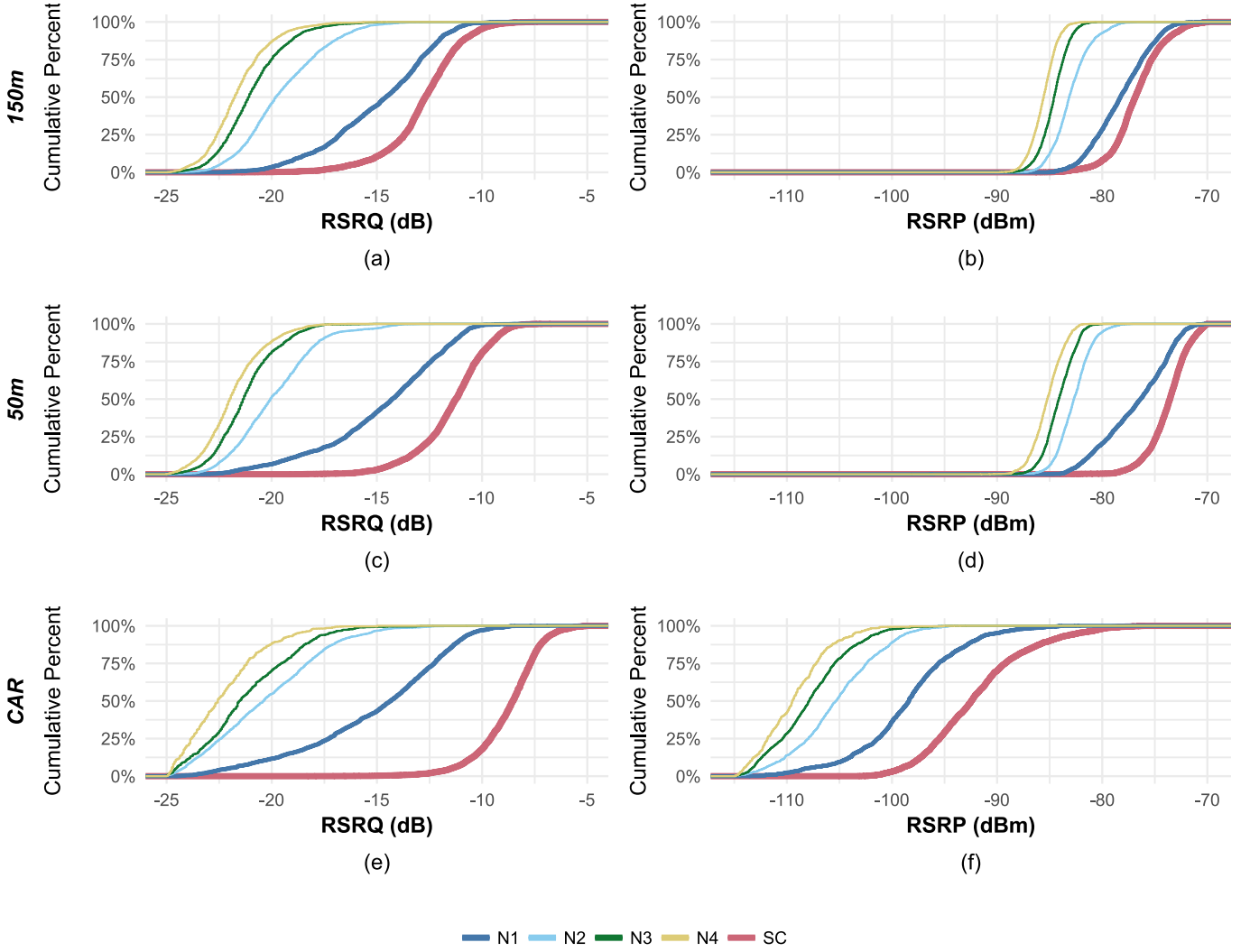


Figure 3: Neighbor cells measurement data: (a), (c), and (e) show distributions of RSRQ at the heights of 150 m and 50 m, and at ground level; (b), (d), and (f) show distributions of RSRP at the heights of 150 m and 50 m, and at ground level. N_k denotes the k -th strongest neighbor cell, and SC denotes the serving cell.

of 50 m or 150 m, the drone user equipment (UE) was likely served by either the low gain parts of the main lobes or the sidelobes of BS antennas, which have reduced antenna gains compared to the main lobes of BS antennas serving UEs at ground level. The propagation conditions in the sky, however, are close to free-space propagation. As a result, we observed that the drone UE experienced stronger serving cell RSRPs than ground UEs.

Reference signal received quality (RSRQ) is a key measurement parameter indicating the received signal quality level in an LTE network. RSRQ includes the effect of interference from neighbor cells. From the RSRQ distributions in Figure 2(b), we can see that RSRQs at the heights of both 50 m and 150 m are lower than the RSRQs at ground level. The 50th percentile RSRQs at the heights of 50 m and 150 m are 2.8 dB and 4.1 dB lower than the corresponding value at ground level, respectively. Worse serving cell RSRQs in the sky are expected due to the close to free-space propagation which leads to stronger downlink interference from non-serving cells to the drone UE.

An alternative received signal quality metric is signal to interference-plus-noise ratio (SINR). Figure 2(c) shows the distributions of reference signal SINR (RS-SINR). The 50th percentile RS-SINRs at the heights of 50 m and 150 m are 7.7 dB and 10.2 dB lower than the corresponding value at ground level, respectively. These RS-SINR results indicate again the much stronger downlink interference from non-serving cells in the sky than at ground level. Note that RSRP, RSRQ, and RS-SINR are all downlink metrics.

Many drone use cases such as flying cameras and remote surveillance are likely to be uplink (from drone UE to BS) data heavy. In the field measurements, we also logged the uplink throughputs over LTE physical uplink shared channel (PUSCH) associated with file uploading, as represented in Figure 2(d). We can see that the variances of uplink throughputs at the heights of both 50 m and 150 m are much smaller than at ground level. We also observe in this field trial that throughputs at the heights of both 50 m and 150 m are higher than the corresponding values at ground level. The 50th percentile throughput at the heights of 50 m and 150 m are ~18.5 Mbps and ~18.8 Mbps, respectively, while the counterpart throughput

at ground level is ~ 12.5 Mbps. In this field trial, the drone UE likely experienced better uplink channel conditions because of close to free-space propagation conditions in the sky when compared to the propagation conditions on the ground. This likely resulted in better uplink throughputs in the sky when compared to the throughputs on the ground. The throughput performance however heavily depends on many factors such as network load and scheduling.

IV. FIELD TRIALS: NEIGHBOR CELL RESULTS AND ANALYSIS

In this section, we examine the field measurement data corresponding to the neighbor cells. The neighbor cell signal strengths and qualities not only can shed light on interference impact but also they are important factors for mobility procedures as UEs are configured to measure and report neighbor cell signal strength and quality values in order for the network to make e.g. handover decisions.

From the field trials, we observe that in general the number of detected neighbor cells increases as the height increases.

- At 5th percentile, the numbers of detected neighbor cells at ground level, at the height of 50 m, and at the height of 150 m are 1, 3, and 3, respectively.
- At 50th percentile, the numbers of detected neighbor cells at ground level, at the height of 50 m, and at the height of 150 m are 3, 5, and 6, respectively.

This trend is expected because as the height increases, more neighbor cells have line-of-sight propagation conditions to the drone UE and thus more cells become detectable.

The distributions of RSRP and RSRQ data for the four strongest neighbor cells are shown in Figure 3. We use N_k to denote the k -th strongest neighbor cell. For ease of comparison, we also plot the distributions of the serving cell RSRP and RSRQ. The first row of plots shows the distributions of RSRP and RSRQ data at the height of 150 m, the second row at the height of 50 m, and the third row at ground level.

From the subfigures (b), (d), and (f) of Figure 3, we can see that the neighbor cell RSRP spread decreases as the height increases. The 50th percentile RSRP difference between the first and the fourth strongest neighbor cell decreases from 11.4 dB at ground level to 7.4 dB at the height of 50 m and to 6.5 dB at the height of 150 m. Further, the difference of the serving cell RSRP distribution and the strongest neighbor cell (i.e., N_1) RSRP distribution at the height of either 50 m or 150 m is much smaller than at ground level. For the neighbor cells other than the first strongest neighbor cell, the 50th percentile RSRPs are below -105 dBm at ground level. However, due to the closer to line-of-sight free-space propagation to the drone UE, the 50th percentile RSRPs of these neighbor cells are above -86 dBm at the height of either 50 m or 150 m. From the subfigures (a), (c), and (e) of Figure 3, we can observe similar trends for RSRQ.

From a UE perspective, its own perceived relative received signal strengths between the detected neighbor cells and serving cell are more relevant. Note that the values of RSRP gaps (serving cell RSRP – neighbor cell RSRP) can be negative since the serving cell is not always the strongest cell in practice due to the dynamic network environment and handover margin used. For the RSRP gap between the serving cell and the first

strongest cell (serving cell RSRP – N_1 RSRP), the percentage of negative RSRP gaps at ground level is $\sim 11\%$ in the field measurement. In contrast, the percentage of negative RSRP gaps increases as the height increases: $\sim 21\%$ at the height of 50 m, and $\sim 33\%$ at the height of 150 m. This is likely due to faster antenna pattern roll-off for the drone UE as it was more often served by either the sidelobe or the main lobe but away from the center of the main lobe of a BS antenna pattern.

In this measurement, we find that the 50th percentile RSRP gaps between the serving cell and the first strongest cell at ground level, at the height of 50 m, and at the height of 150 m are 6.5 dB, 2.8 dB, and 1.6 dB, respectively. A typical measurement report triggering condition is that when a neighbor cell becomes X dB better than the serving cell, where X is usually set to a small value (e.g. 3 dB). From the field measurement data, we can see that the RSRP gap between the serving cell and the first strongest cell becomes more reduced as the height increases. If the network can detect that the UE is flying, network may apply different configurations, e.g. for measurements for the UE, and have different criteria for handover decisions.

V. SIMULATIONS: LATENCY RESULTS AND ANALYSIS

Field trials are valuable but they are also limited in terms of number of drones that can be simultaneously tested and the range of features and configurations in an operational commercial network. To complement field trials, we performed simulations to gain insights into the network performance when the network is serving many drone UEs simultaneously over a wide area.

The ability of remote command and control can significantly enhance the safety and operation of drones. Such command and control communications need to be reliable, and the packets should be successfully delivered within some latency bound (depending on the use case) with high probability. In this section, we present simulation results of radio interface latency for LTE networks serving command and control traffic for drones.

A. Simulation Setup

The latency simulation assumptions follow the 3GPP study item on enhanced LTE support for aerial vehicles [13]. For ease of reference, we summarize a few key evaluation assumptions in the sequel.

- Traffic model: packets arrive periodically with a period of 100 ms and a fixed packet size of 1250 bytes, which leads to a data rate of 100 kbps for command and control at each drone UE. The required latency bound is 50 ms.
- Deployment scenario: an urban macro scenario with aerial vehicles (UMa-AV), where sites are placed on a hexagonal grid with 19 sites and 3 cells per site. The LTE system bandwidth is 10 MHz at 2 GHz carrier frequency.
- Antenna model and configuration: Each BS has two cross polarized TX/RX antennas with 10 degrees of downtilt at the height of 25 m. The BS antennas are modeled by a synthesized antenna pattern using an antenna array with a column of 16 cross-polarized antenna elements, where the

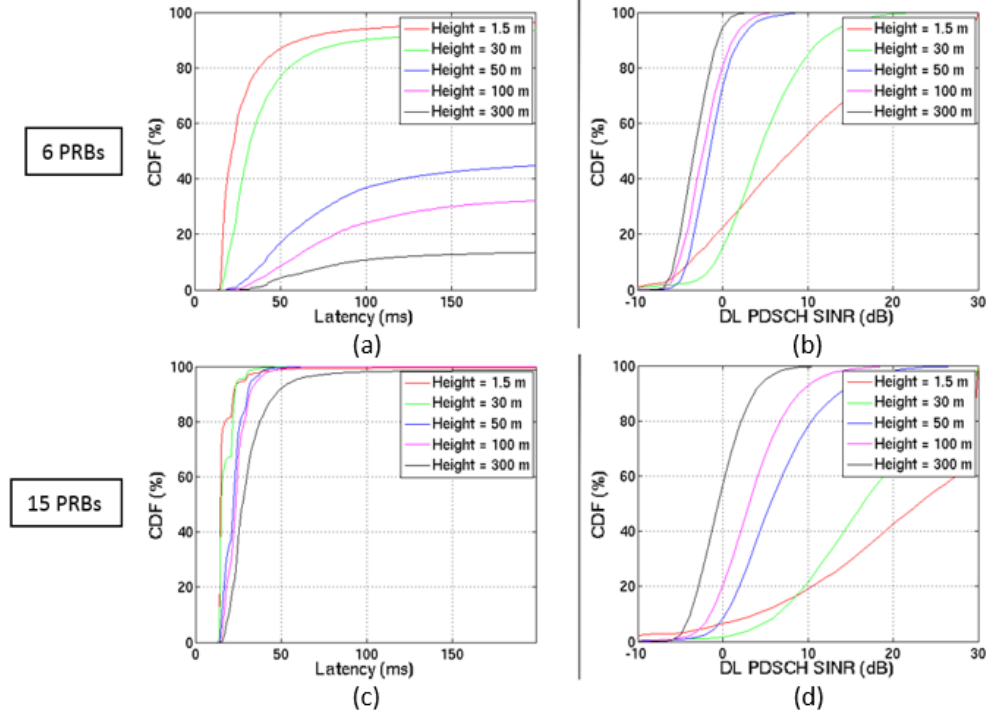


Figure 4: Downlink latency simulation results: (a) and (c) show latency distributions when 6 and 15 PRBs are used to serve drone UEs, respectively; (b) and (d) show PDSCH SINR distributions when 6 and 15 PRBs are used to serve drone UEs, respectively.

antenna spacing is 0.8λ where λ denotes the wavelength. Each UE has one omni-directional TX and two cross-polarized omni-directional RXs.

In this evaluation, we focus on command and control traffic in the downlink and assume that the scheduler partitions the radio resources so that the drone traffic and terrestrial mobile traffic are scheduled in orthogonal frequency resources. With this partition, the signals to terrestrial UEs and the signals to drone UEs do not interfere. However, drone UEs in a cell still experience interference from neighbor cells since the neighbor cells may use the same radio resource to serve other drone UEs connected to the neighbor cells.

We assume 5 drone UEs in each cell, resulting in 500 kbps command and control traffic demand per cell. In the evaluation, we simulated the performance at different heights: 1.5 m, 30 m, 50 m, 100 m, and 300 m. We present simulation results below under 2 different numbers of physical resource blocks (PRBs) used for drone UEs: 6 PRBs (i.e., 1.08 MHz) and 15 PRBs (i.e., 2.7 MHz). The results will show the tradeoff between latency performance and the number of PRBs used for command and control.

B. Number of PRBs Used for Connected Drones: 6

Figure 4(a) shows the latency distributions at different heights when 6 PRBs are used to serve the drone traffic. Figure 4(b) shows the corresponding SINR distributions of physical downlink shared channel (PDSCH).

From the distributions of PDSCH SINR, we can see that SINR drops significantly as the height increases, especially for the heights equal to or higher than 50 m. From the latency distributions, we can see that even at ground level of 1.5 m, it is not possible to meet the 50 ms latency bound with a high confidence level (e.g. 90%).

To better understand the results, we next examine the resource utilization ratios. The resource utilization ratio is defined as the fraction of utilized radio resources averaged over time, frequency, and cells. It is a key performance indicator that can reflect the interference level in the network.

When 6 PRBs are used to serve the drone traffic, we find that the resource utilization ratios are ~41%, ~57%, ~90%, ~95%, and ~96% at the heights of 1.5 m, 30 m, 50 m, 100 m, and 300 m, respectively. These resource utilization ratios help explain the results. At ground level of 1.5 m, the resource utilization is already ~41%, which implies that close to half of the BSs are transmitting and a typical drone UE receiving a downlink packet experiences interference from the corresponding active neighbor cells. As the height increases to 50 m, the resource utilization becomes ~90%, and increases further to ~95% as the height further increases. In other words, almost all the BSs are transmitting and a typical drone UE at the height of 50 m or above experiences strong inter-cell interference. The increased resource utilization in the sky is due to poor geometry which in turn leads to lower spectral efficiency because of interference.

In conclusion, without additional techniques for interference mitigation, serving the drone command and control traffic demand of 500 kbps per cell with 6 PRBs to meet a tight latency bound is challenging.

C. Number of PRBs Used for Connected Drones: 15

Figure 4(c) shows the latency distributions at different heights when 15 PRBs are used to serve the drone traffic. Figure 4(d) shows the corresponding distributions of PDSCH SINR.

From the distributions of PDSCH SINR, we can see that though SINR drops significantly as the height increases, it is much higher than the case when only 6 PRBs are used to serve the drone traffic. From the latency distributions, we can see that

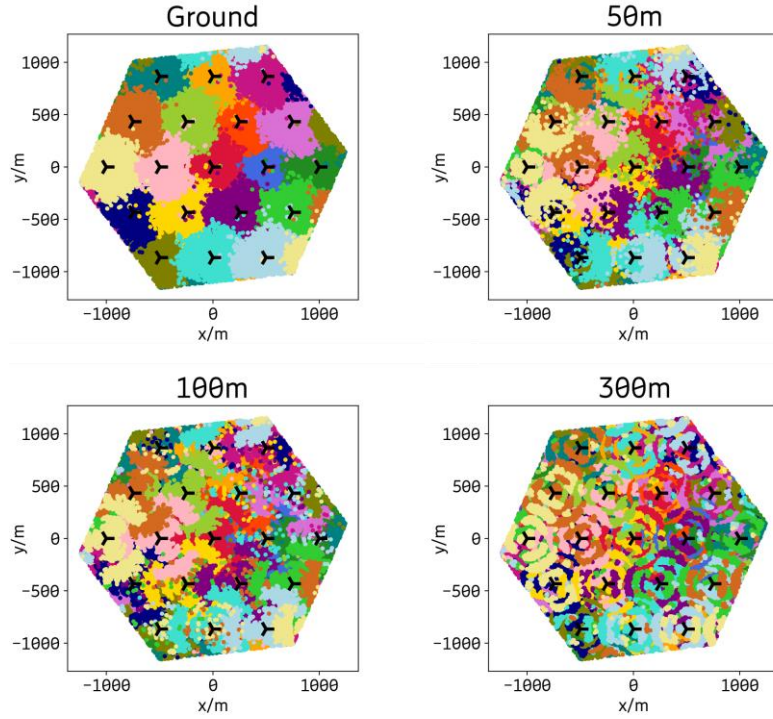


Figure 5: Maximum received power based cell association patterns at ground level and at the heights of 50 m, 100 m, and 300 m: UEs in the areas marked by the same color are associated with the same site.

it is possible to meet the 50 ms latency bound with a high confidence level ($\sim 99\%$) at 1.5 m, 30 m, 50 m, and 100 m, and $\sim 92\%$ probability at 300 m.

When 15 PRBs are used to serve the drone traffic, we find that the resource utilization ratios are $\sim 11\%$, $\sim 11\%$, $\sim 23\%$, $\sim 30\%$, and $\sim 47\%$ at the heights of 1.5 m, 30 m, 50 m, 100 m, and 300 m, respectively. These resource utilization ratios help explain the results. At the height of 1.5 m, 30 m, 50 m, or 100 m, the resource utilization is not larger than $\sim 30\%$, and thus the downlink interference experienced at drone UEs is moderate. At the height of 300 m, the resource utilization is $\sim 47\%$, and thus the downlink interference is stronger.

D. Remarks on the Latency Results

The above results show the tradeoff between latency performance and the number of PRBs used for drone command and control traffic. Note that the results are under a high command and control traffic demand: 5 drone UEs per cell and each has periodic packet arrivals with a fixed packet size of 1250 bytes and a period of 100 ms. In the initial phase of drone deployment, it is likely that the demand of command and control traffic is much lower.

A general trend we observe from the resource utilization ratios is that as the height increases from 30 m to 300 m, the resource utilization increases for the same offered command and control traffic. For example, when 15 PRBs are used to serve the traffic, to meet the 50 ms latency bound with $\sim 99\%$ confidence level, the resource utilization ratio is increased by $\sim 2x$ when the height increases from 30 m to 50 m, and $\sim 3x$ when the height increases from 30 m to 100 m.

A key lesson from the above results is that when the resource utilization ratio is low, the downlink interference experienced at drone UEs is not strong, which makes it possible to deliver a

small data packet within the 50 ms latency bound with a high confidence level. It is expected that as long as an interference mitigation technique can lead to satisfactory SINR values, it is possible to deliver a small command and control packet within some latency bound with a high confidence level. Several interference mitigation solutions were identified in 3GPP study item on enhanced LTE support for connected drones [13].

VI. SIMULATIONS: MOBILITY RESULTS AND ANALYSIS

Ensuring reliable connections in the presence of drone movements is important for many drone use cases. With increasing height above the ground, the radio environment changes. Using existing mobility management mechanisms in LTE networks to provide connectivity to the drones moving in the sky may face new challenges.

There are two main aspects that make mobility support for drone UEs challenging. First is the serving cell signal. BS antennas are typically tilted downwards by a few degrees. The main lobe of a BS antenna thus covers a large part of the surface area of the cell to improve performance for terrestrial UEs. Accordingly, at ground level the strongest site is typically the closest one. A drone UE on the other hand may be frequently served by the sidelobes of BS antennas, which have lower antenna gains. The coverage areas of the sidelobes may be small and the signals at the edges may drop sharply due to deep antenna nulls. At a given location, the strongest signal might come from a faraway BS, if the gain of the sidelobes of the closer BSs to the drone UE is much weaker. These effects can be clearly seen in Figure 5, which shows the maximum received power based cell association patterns at ground level and at the heights of 50 m, 100 m, and 300 m. At the higher heights, the

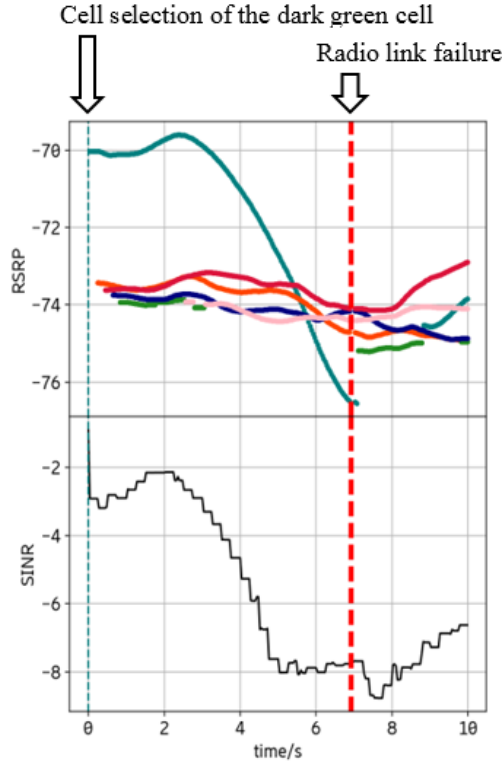


Figure 6: An example mobility trace for a drone UE moving away from the coverage of a BS antenna sidelobe at the speed of 30 km/h and at the height of 300 m: Each colored RSRP trace corresponds to one cell.

coverage areas become fragmented and the fragmentation pattern is determined by the lobe structures of the BS antennas.

The second aspect is interference. As pointed out previously, as the height increases, more BSs have line-of-sight propagation conditions to drone UEs. As a result, the drone UEs may generate more uplink interference to the neighbor cells while experiencing more downlink interference from the neighbor cells. Due to the increased interference, SINR could become quite poor at certain heights. Degraded SINR might lead to more radio link failures. It might also result in more handover failures since measurement reports, handover commands, etc., may get lost during the handover execution procedure.

To illustrate the challenges of mobility support for drone UEs, Figure 6 shows an example mobility trace for a drone UE moving away from the coverage of a BS antenna sidelobe at the speed of 30 km/h and at the height of 300 m. The upper subfigure of Figure 6 shows the RSRP measurements by the drone UE, and the bottom subfigure shows the time varying trace of the serving cell SINR. Each colored RSRP trace corresponds to one cell. In Figure 6, the vertical dark green dashed line at the beginning marks cell selection of the dark green cell. At about 3 s, the serving cell RSRP begins to drop, and it drops by 7 dB within 4 s. After 5 s the neighboring cells become stronger than the serving cell. However, to trigger handover measurement reports, some neighbor cell RSRP should be X dB better than the serving cell, where X is set to 3 in the simulation. From the RSRP traces, we can see that the RSRPs of the neighbor cells stay relatively low, and none of

them is at least 3 dB better than the serving cell before the drone UE declares radio link failure at $t = 7$ s (marked by the vertical red dashed line) due to poor serving cell SINR.

To sum up, Figure 6 illustrates the two main aspects that make mobility support for flying drone UEs challenging and interesting: serving cell signal and interference. Since drone UEs that are flying may be served by the sidelobes of BS antennas, they might experience sudden drops in signal quality due to antenna nulls when they move from the coverage area of one sidelobe to the coverage area of another sidelobe. The default handover procedure may become too slow to be successfully executed. Further, we can see from Figure 6 that the gaps between the serving cell RSRP and the neighbor cell RSRPs are small. The strong interference from neighbor cells makes the serving cell SINR stay relatively low throughout.

As it has become evident that signal strength conditions are different when a UE is flying and when the UE is on the ground, it becomes important for the network to detect when the UE is flying. This has been discussed during the study item phase in 3GPP [13] and is going to be addressed in the work item phase as well [15]. The proposed solutions vary from UE informing the network with a flying mode status to network detecting whether the UE is flying based on different variables such as timing advance or measurement reports. In some solutions, measurements are triggered under conditions that likely match to flying mode. Currently an LTE UE does not indicate a mode, such as a flying mode, or speed or position to network autonomously but this kind of information may be piggy-backed in mobility measurement report. Alternatively, the network could poll the UE when it suspects that UE could be flying. To follow the principle that UEs would not autonomously send indications to network, as that may cause unwanted and uncontrollable uplink traffic, a combination of detecting a likely flying mode from other parameters such as measurement reports possibly following by polling UE with flight mode status could serve as solution to enable the network to recognize drone UEs that are flying. After network has detected a flying drone UE, the UE may be configured with a measurement configuration that better fits to signal strength and quality patterns experienced in flying mode and thus network may also prepare for handovers more suitable in this situation. For example, handover may be executed to a further away cell instead of to a close neighbor.

VII. CONCLUSIONS

Mobile networks have connected tens of billions of devices on the ground in the past decades and are now ready to power the flying drones in the sky. Wide-area, high speed, and secure wireless connectivity provided by mobile networks can enhance safe operation and management of the growing fleet of drones in a wide variety of industries and services. The field trial and simulation results, analysis, and design insights presented in this article shed light on the applicability and performance of mobile network connectivity to low altitude drones. We find that the existing mobile LTE networks targeting terrestrial usage can support the initial deployment of low altitude drones, but there may be challenges related to interference as well as mobility. Enhancements including those identified in the 3GPP technical report [13] and the next generation 5G networks will

provide more efficient connectivity for wide-scale drone deployments. It will be a long road ahead to truly unlock drones' full potential by overcoming technology challenges together with advances in regulatory, policy, and business considerations. We hope that this article will help to pave the way for the internet of drones.

http://www.3gpp.org/ftp/TSG_RAN/TSG_RAN/TSGR_78/Docs/RP-172826.zip. Accessed on January 30, 2018.

REFERENCES

- [1] Amazon, "Prime air." Online: <https://www.amazon.com/Amazon-Prime-Air/b?node=8037720011>. Accessed on January 30, 2018.
- [2] Goldman Sachs, "Drones: Reporting for work," 2017. Online: <http://www.goldmansachs.com/our-thinking/technology-driving-innovation/drones/>. Accessed on January 30, 2018.
- [3] SESAR, "European drones outlook study," November 2016. Online: http://www.sesarju.eu/sites/default/files/documents/reports/European_Drones_Outlook_Study_2016.pdf. Accessed on January 30, 2018.
- [4] M. Gharibi, R. Boutaba and S. L. Waslander, "Internet of drones," *IEEE Access*, vol. 4, pp. 1148-1162, March 2016.
- [5] S. Shariatmadari *et al*, "Designing and implementing future aerial communication networks," *IEEE Communications Magazine*, vol. 54, no. 5, pp. 26-34, May 2016.
- [6] FAA, "UAS traffic management research transition team plan," *technical report*, January 2017. Online: https://www.faa.gov/uas/research/utm/media/FAA_NASA_UAS_Traffic_Management_Research_Plan.pdf. Accessed on January 30, 2018.
- [7] U.S. DOT and FAA, "UAS integration pilot program," October 2017. Online: https://www.faa.gov/uas/programs_partnerships/uas_integration_pilot_program/. Accessed on January 30, 2018.
- [8] D. W. Matolak and R. Sun, "Unmanned aircraft systems: Air-ground channel characterization for future applications," *IEEE Vehicular Technology Magazine*, vol. 10, no. 2, pp. 79-85, June 2015.
- [9] B. V. Der Bergh, A. Chiumento and S. Pollin, "LTE in the sky: Trading off propagation benefits with interference costs for aerial nodes," *IEEE Communications Magazine*, vol. 54, no. 5, pp. 44-50, May 2016.
- [10] M. Mozaffari, W. Saad, M. Bennis and M. Debbah, "Wireless communication using unmanned aerial vehicles (UAVs): Optimal transport theory for hover time optimization," *IEEE Transactions on Wireless Communications*, vol. 16, no. 12, pp. 8052-8066, December 2017.
- [11] GSMA, "Mobile spectrum for unmanned aerial vehicles; GSMA public policy position," *white paper*, October 2017. Online: <https://www.gsma.com/spectrum/wp-content/uploads/2017/10/Mobile-spectrum-for-Unmanned-Aerial-Vehicles.pdf>. Accessed on January 30, 2018.
- [12] 3GPP RP-170779, "Study on enhanced LTE support for aerial vehicles," NTT DOCOMO, Ericsson, March 2017. Online: http://www.3gpp.org/ftp/tsg_ran/tsg_ran/TSGR_75/Docs/RP-170779.zip. Accessed on January 30, 2018.
- [13] 3GPP TR 36.777, "Enhanced LTE support for aerial vehicles," Online: ftp://www.3gpp.org/specs/archive/36_series/36.777. Accessed on January 30, 2018.
- [14] X. Lin, V. Yajnanarayana, S. D. Muruganathan, S. Gao, H. Asplund, H.-L. Maattanen, M. Bergström A, S. Euler, Y.-P. E. Wang, "The sky is not the limit: LTE for unmanned aerial vehicles," to appear in *IEEE Communications Magazine*, July 2017. Available at arXiv:1707.07534.
- [15] 3GPP RP-172826 "New WID on Enhanced LTE Support for Aerial Vehicles," Ericsson, December 2017. Online: